Transient Modeling and Controlling of a New Topology of UPFC for Transmission System Applications

Ali Ajami[1], Non-member

ABSTRACT

The theory, transient and steady state models of a new topology of UPFC, the center node unified power flow controller(C-UPFC), are presented in this paper. Also, a control system for this device is presented. The CUPFC consists of three voltage source inverters (VSI) with common DC link capacitor. The proposed model represents the behavior of the controller in the steady and transient states operating conditions. The presented model and control system of C-UPFC is validated with help of the PSCAD/EMTDC simulation program. In this paper C-UPFC is simulated under different operating conditions. The presented control system enables the CUPFC to independent control of the active and reactive power flows at the both ends of transmission line, regulating the DC link capacitor and AC bus voltage and power oscillation damping. It will be shown that by adding a supplementary control signal to the shunt inverter control system, it is possible to balance line current too.

Keywords: FACTS, Transient Model, Transient Stability, UPFC, C-UPFC, Line Current Balancing

1. INTRODUCTION

The concept of the flexible AC transmission systems (FACTS) based on the power electronics converters has introduced many possibilities for fast controlling and optimization of electric power flow in transmission lines and improving the power quality of distribution subsystems [1]. The FACTS devices can be categorized as:

Transformer based devices (e.g., Inter Phase Controllers) [2].

Thyristor based devices (e.g., Thyristor Controlled Series Capacitor) [3].

Self commutated based devices (e.g., STATIC Compensator [4], Static Synchronous Series Compensator [5, 6], Unified Power Flow Controller [7, 8]).

The UPFC is the most elegant device of FACTS controllers, shown in Fig. 1. It consists of two voltage source converters with one common DC link capacitor. The converters are connected in parallel and in series. Each converter can independently generate or absorb reactive power. This arrangement enables control of active and reactive power. The ordinary UPFC has 4 control variables (phase and magnitude of shunt and series converters). Using these control variables it is possible to control the line active power flow, sending or receiving end reactive power, shunt converter AC bus voltage and DC link voltage [9, 10]. Because of the limited number of control variables, the ordinary UPFC is not capable of controlling the line active and reactive powers of two machine system, simultaneously. To overcome this problem, a new topology of UPFC has been used. This new FACTS device is named center node UPFC (C-UPFC) installed at the midpoint of transmission line [11]. The proposed device consists of three IGCT based voltage source converters (see Fig.2). A shunt converter is connected at the midpoint of two series connected converters. In this paper the capabilities of this device will be discussed. It will be shown that this device can control the active and reactive powers of receiving and sending ends and simultaneously can regulate the midpoint voltage magnitude and DC link voltage. Also, in [11] C-UPFC with 2 DC links is presented for the steady state applications. In this paper the transient model of CUPFC and its application for the line current balancing is presented and the suggested device needs only one DC link.

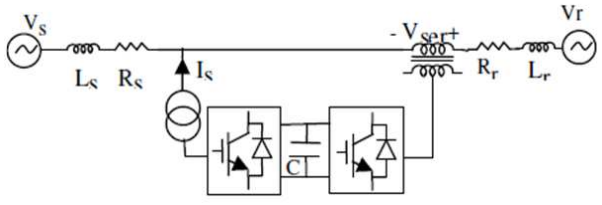

Fig.1: *General configuration of UPFC*

2. MODELING OF C-UPFC

2.1 Steady State Model

The single line diagram of the C-UPFC fundamental frequency model is illustrated in Fig.3-a. In this model the losses are neglected.

Manuscript received on January 25, 2010 ; revised on October 4, 2010.

[1] The author is with Electrical Engineering Department of Azerbaijan University of Tarbiat Moallem, Tabriz, Iran, E-mail: ajami@azaruniv.edu

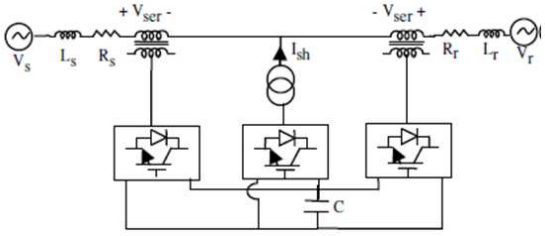

Fig.2: *General configuration of C-UPFC*

Fig. 3-b and c show the phasor diagrams of transmission line without and with installed C-UPFC. The DC link voltage and AC mid point voltage (Vo) are controlled and regulated by shunt inverter.

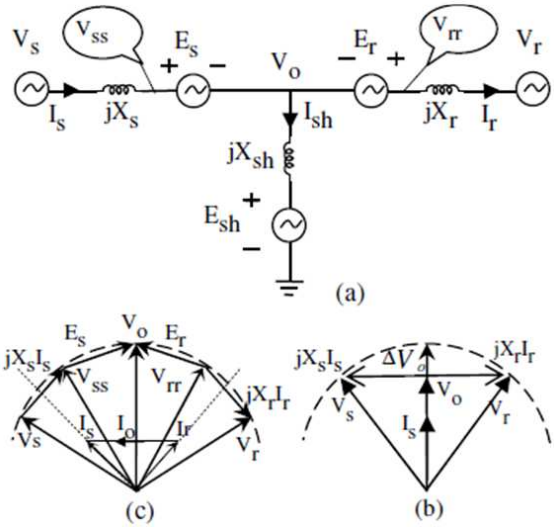

Fig.3: *Phasor diagram of transmission line a- The fundamental frequency model of C-UPFC b- without C-UPFC c- with C-UPFC*

With regulating mid point voltage and controlling the magnitude and phase of series inverters voltages the phase and magnitude of Vrr and Vss can be controlled independently and therefore, active and reactive power of both ends machine are controlled independently. Hence, the presented topology of UPFC has 6 control variables.

The main objective of series inverters is to produce AC voltages of controllable magnitude and phase angle, and inject these voltages at fundamental frequency into the transmission line. Therefore, the real and reactive power of both ends of transmission line is controlled as independently. The shunt converter provides the required real power at the DC terminals. Also, the shunt inverter controls AC bus voltage by generating/ absorbing of reactive power.

2.2 Transient Model of C-UPFC

Fig.4 shows the transient model of the C-UPFC. The L_{sh}, L_{sr_s}, $L_{sr\text{-}r}$ and R_{sh}, $R_{sr\text{-}s}$, $R_{sr\text{-}r}$ represent leakage inductances of transformers and losses of inverters and transformers. The shunt converter of C-UPFC operates like a STATCOM [12]. It provides the path for the shunt current ($II_{sh} = I_s - I_r$) and sets the midpoint voltage magnitude on $|V_r| = |V_s| = |V_o|$.

$$\begin{bmatrix} V_{shd} \\ V_{shq} \end{bmatrix} = \begin{bmatrix} N_{sh}V_{md} - R_{sh}I_{sh1d} - L_{sh}\frac{d}{dt}I_{sh1d} - \omega L_{sh}I_{sh1d} \\ N_{sh}V_{mq} - R_{sh}I_{sh1q} - L_{sh}\frac{d}{dt}I_{sh1q} - \omega L_{sh}I_{sh1q} \end{bmatrix} \quad (1)$$

$$\begin{bmatrix} V_{sr\_sd} \\ V_{sr\_sq} \end{bmatrix} = \begin{bmatrix} N_{sr\_s}(V_{msd}-V_{md}) + R_{sr\_s}I_{sr_sd} + I_{sr\_s}\frac{d}{dt}I_{sr\_sd} - \omega L_{sr_s}I_{sr_sd} \\ N_{sr\_s}(V_{msq}-V_{md}) + R_{sr\_s}I_{sr_sq} + I_{sr\_s}\frac{d}{dt}I_{sr\_sq} - \omega L_{sr_s}I_{sr_sq} \end{bmatrix} \quad (2)$$

$$\begin{bmatrix} V_{sr\_rd} \\ V_{sr\_rq} \end{bmatrix} = \begin{bmatrix} N_{sr\_r}(V_{mrd}-V_{md}) + R_{sr\_r}I_{sr_rd} + L_{sr\_r}\frac{d}{dt}I_{sr\_rd} - \omega L_{sr_r}I_{sr_rd} \\ N_{sr\_r}(V_{msq}-V_{md}) + R_{sr\_s}I_{sr_sq} + L_{sr\_r}\frac{d}{dt}I_{sr\_rq} - \omega L_{sr_r}I_{sr_rq} \end{bmatrix} \quad (3)$$

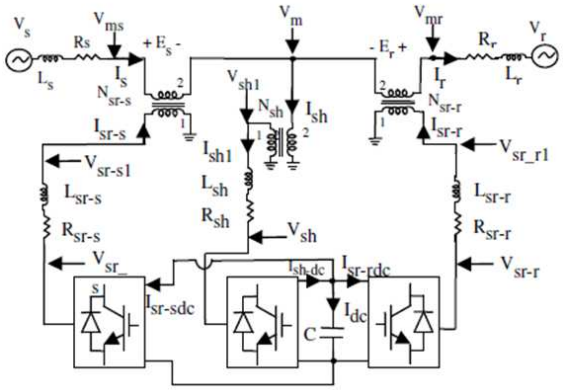

Fig.4: *Transient model of C-UPFC*

3. CONTROL STRATEGY OF CONVERTERS

In most cases, the UPFC is used to control its sending end bus voltage magnitude by generating or absorbing reactive power, and to control power flows on the transmission line by regulating the magnitude and phase angle of series injected voltage. This control mode is named automatic voltage and power flow control mode. In this paper, this and power/ frequency oscillation damping mode for C-UPFC are presented.

3.1 Series Inverters

By controlling the magnitude and phase angle of line current, active and reactive power of sending and receiving ends can be controlled. The line current can be controlled by injection of series voltages, Es and Er.The sending and receiving ends active and reactive powers are calculated by equations (4) and (5).

$$\begin{bmatrix} P_s \\ Q_s \end{bmatrix} = \frac{3}{2} \begin{bmatrix} V_{sd} & V_{sq} \\ -V_{sq} & V_{sd} \end{bmatrix} \begin{bmatrix} I_{sd} \\ I_{sq} \end{bmatrix} \quad (4)$$

$$\begin{bmatrix} P_r \\ Q_r \end{bmatrix} = \frac{3}{2} \begin{bmatrix} V_{rd} & V_{rq} \\ -V_{rq} & V_{rd} \end{bmatrix} \begin{bmatrix} I_{rd} \\ I_{rq} \end{bmatrix} \quad (5)$$

The real power flow from sending and receiving ends can be independently controlled if the DC link is a DC voltage source. In this paper DC link is only a capacitor. Neglecting the line and inverters losses we have:

$$P_r = P_s = P \quad (6)$$

The reference currents of series inverters are obtained from equations (4) and (5) as bellow:

$$\begin{bmatrix} I^*_{sr\_s1d} \\ I^*_{sr\_s1q} \end{bmatrix} = \frac{2}{3} \frac{N_{sr\_s}}{(V^2_{sd} + V^2_{sq})} \begin{bmatrix} V_{sd} & -V_{sq} \\ V_{sq} & V_{sd} \end{bmatrix} \begin{bmatrix} P^* \\ Q^*_s \end{bmatrix} \quad (7)$$

$$\begin{bmatrix} I^*_{sr\_r1d} \\ I^*_{sr\_r1q} \end{bmatrix} = \frac{2}{3} \frac{N_{sr\_r}}{(V^2_{rd} + V^2_{rq})} \begin{bmatrix} V_{rd} & -V_{rq} \\ V_{rq} & V_{rd} \end{bmatrix} \begin{bmatrix} P^* \\ Q^*_r \end{bmatrix} \quad (8)$$

Considering equations 2, 3, 7 and 8 the control system of series inverters can be formed as Fig. 5.

3.2 Shunt Inverter

The shunt converter has basically two functions:

1- Controlling the voltage magnitude at the sending end bus by generating or absorbing reactive power.

2- Supplying the demanded real power at the DC terminal by series inverters.

With controlling reactive power of shunt inverter the midpoint bus voltage is controlled. Qsh can be calculated as follows:

$$Q_{sh} = \frac{3}{2} (V_{md} I_{shq} - V_{mq} I_{shd}) \quad (9)$$

The exchanged active power between series inverters and AC system is caused to change the DC link voltage. Therefore, the shunt inverter must supply the active power of series inverters, P_{sr}, and the losses of three inverters, Ploss, to regulate the DC link voltage. P_{sr} can be calculated as follows:

$$P_{sr} = \frac{3}{2}(E_{sd} I_{sd} + E_{sq} I_{sq}) - \frac{3}{2}(E_{rd} I_{rd} + E_{eq} I_{rq}) \quad (10)$$

The active power of shunt inverter can be written as follows:

$$P_{sh} = P_{sr} + P_{loss} = \frac{3}{2}(V_{md} I_{shd} + V_{mq} I_{shq}) \quad (11)$$

Using equations (9), (11) and turn ratio of shunt transformer the reference currents of shunt inverter can be obtained as bellow:

$$\begin{bmatrix} I_{sh1d} \\ I_{sh1q} \end{bmatrix} = \frac{2}{3} N_{sh} \frac{1}{(V^2_{md} + V^2_{mq})} \begin{bmatrix} V_{md} & -V_{mq} \\ V_{mq} & V_{md} \end{bmatrix} \begin{bmatrix} P_{sh} \\ Q_{sh} \end{bmatrix} \quad (12)$$

The shunt converter can be used to balance the line current and to compensate line current harmonics. Therefore a supplementary control signal must be added to the control system of shunt converter. To obtain this signal, the active, P, and reactive, Q, powers of the load side are calculated.

$$P = \tilde{P} + \bar{P} = \frac{3}{2} (V_{md} I_{rd} + V_{mq} I_{rq}) \quad (13)$$

$$Q = \tilde{Q} + \bar{Q} = \frac{3}{2} (V_{md} I_{rq} - V_{mq} I_{rd}) \quad (14)$$

The unbalance current of load can be obtained as follows:

$$I_{unbal} = \frac{1}{3} (I_{La} + I_{Lb} + I_{Lc}) \quad (15)$$

The desired value of $\tilde{Q}, \bar{Q}, P$ and I_{unbal} is equal to zero. Therefore, the shunt branch must compensate these parameters. To extract undesired component of active power, i.e. $\tilde{P}$, the instantaneous active power signal must pass through a high pass filter with a cut off frequency of 10 Hz. The d-q forms of the supplementary reference signal of shunt branch current are calculated using equations (16) and (17).

$$I^*_d = \frac{\tilde{P} V_{md} - Q V_{mq}}{V^2_{md} + V^2_{mq}} \quad (16)$$

$$I^*_q = \frac{\tilde{P} V_{mq} - Q V_{md}}{V^2_{md} + V^2_{mq}} \quad (17)$$

Now, they must be added to equation (12) (see equation 18).

$$\begin{bmatrix} I_{sh1d} \\ I_{sh1q} \end{bmatrix} = \frac{2}{3} N_{sh} \left\{ \frac{1}{(V^2_{md} + V^2_{mq})} \begin{bmatrix} V_{md} & -V_{mq} \\ V_{mq} & V_{md} \end{bmatrix} \begin{bmatrix} P_{sh} \\ Q_{sh} \end{bmatrix} + \begin{bmatrix} I^*_d \\ I^*_q \end{bmatrix} \right\} \quad (18)$$

The reference currents of shunt inverter can be obtained by:

$$\begin{bmatrix} I^*_{sha} \\ I^*_{shb} \\ I^*_{shc} \end{bmatrix} = T(\theta)^{-1} \begin{bmatrix} I_{sh1d} \\ I_{sh1q} \\ I_{unbal} \end{bmatrix} + \begin{bmatrix} I_{unbal} \\ I_{unbal} \\ I_{unbal} \end{bmatrix} \quad (19)$$

Fig.6 shows the control system of this inverter. To consider the losses of inverters the DC link voltage error must be added to this control system.

$$V_{dcerr} = V^*_{dc} - V_{dc} \quad (20)$$

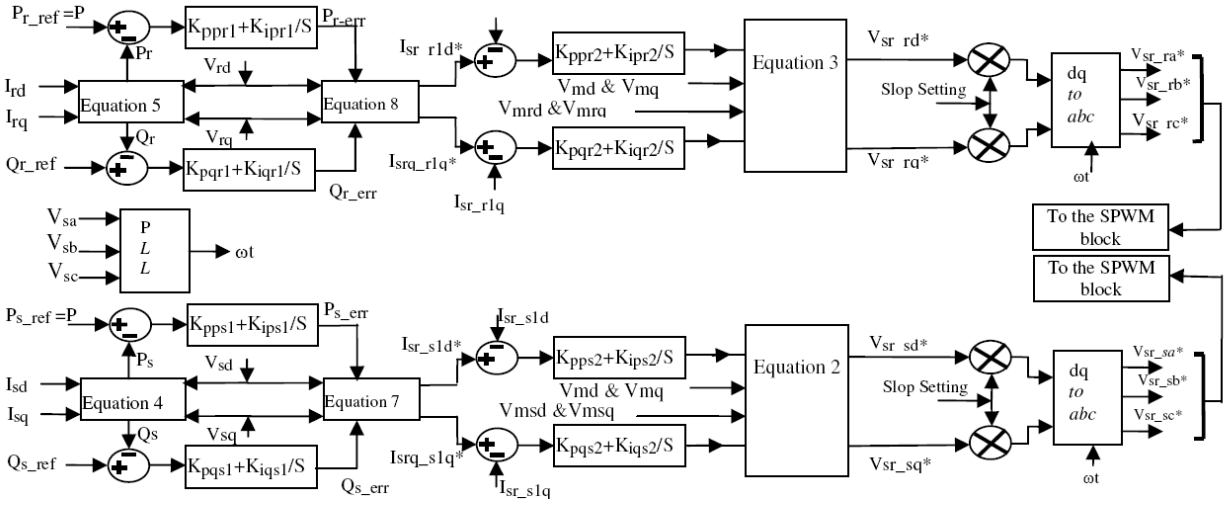

Fig.5: *Control system of series inverters*

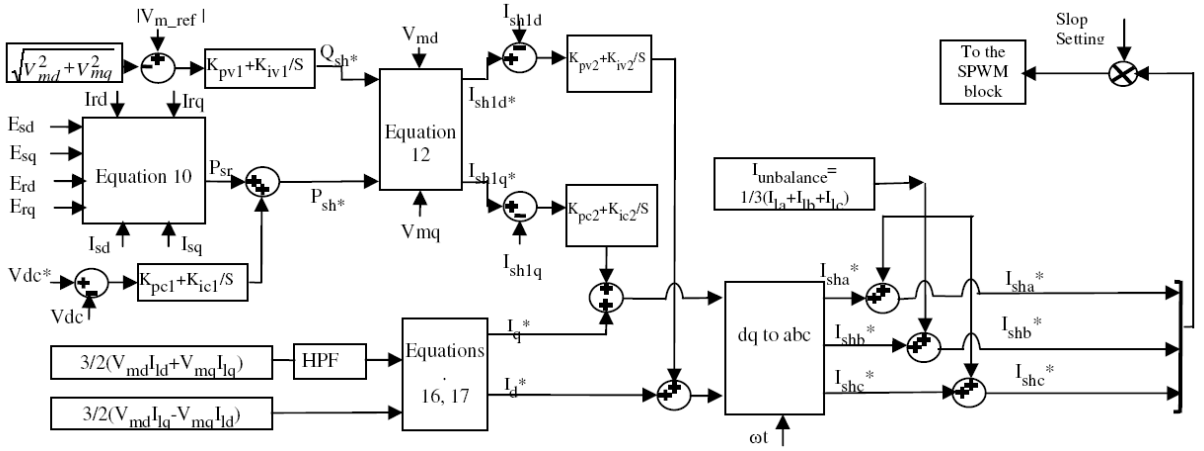

Fig.6: *Control system of shunt inverter*

3.3 Power Oscillation Damping

In the presented control system for power oscillation damping, see Fig. 7, the rotor speed variation directly is added to active power reference signal, Pref, at series converters control systems. The simulation results carried out by transient model, show that the power oscillations caused by 3 and 1 phase fault are quickly controlled. The generator phase angle oscillations are damped faster and hence the system appears to be more stable.

4. SWITCHING STRATEGY OF CONVERTERS

The C-UPFC is consists of three voltage source converters with semiconductor devices having turn off capability. There are two basic control strategies that can be used to control the switching of semiconductor switches in the converters [16].

1- Pulse Width Modulation (PWM) method.

2- Phase Control Strategy.

GTO switches operate adequately at the low switching frequencies required in phase control, but present losses at the high switching frequencies needed for PWM control. However, recent advances in high voltage IGBT technology have led to the development of the Integrated Gate Commutated Thyristor (IGCT), which is basically an optimum combination of thyristor and GTO technology at low cast, low complexity and high efficiency [17]. It can handle higher switching frequencies with relatively low losses, allowing for the practical implementation of PWM control methodologies.

In the phase control approach in order to generating the output voltage waveforms with low harmonics, must be used multi connected phase shifted converters with a common DC link and coupled through appropriate magnetic circuits.

The PWM technique is based on fast switching of semiconductor switches to produce an output voltage waveform with low harmonic, which depends on

the number of notches per cycle. The advantage of this technique is that it allows independent and easy control of active and reactive power components, provided that the DC voltage is kept constant and sufficiently high.

In this paper, the closed loop Sinusoidal PWM controller is used. Fig. 8 shows the gate pulse generator circuit of the series and shunt inverters based on SPWM technique. In the presented SPWM technique, the error signal is applied to a proportional controller and the output signal of controller is the reference signal of SPWM technique.

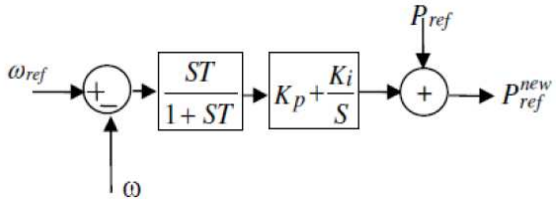

Fig.7: *Power oscillation damping controller*

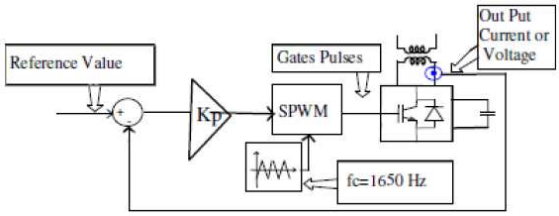

Fig.8: *Generator circuit of gate pulses*

5. SIMULATION RESULTS

The two machine test system, whish is simulated by PSCAD/EMTDC [18], is shown in Fig.9. The inverters consist of IGCT based three phase voltage source converters. The transmission line configuration is illustrated in Fig. 10. The parameters of test system are listed in appendix. The C-UPFC is located at the mid point of transmission line to control the power flow and transient stability enhancement. The power system is subjected to different perturbations to simulate the presented transient model and control system of C-UPFC. Thus, the following cases are studied on the test system:

The active and reactive power references of line are changed as step.

The load angle of generator is changed as step.

An unbalance load is added to the mid point bus.

A 3-phase fault through impedance is applied.

Finally, the C-UPFC is used to damping the out put power oscillations of generator caused by the 3 and one phase fault.

As mentioned earlier, the C-UPFC can control line active and reactive power flows in steady state and transient conditions. Fig. 11 shows the reference and line active power flows. As it can be seen the line power flow follows the step changes of reference. To compare the capability of UPFC and C-UPFC, the Fig. 12-a and b show the reactive powers of receiving and sending ends, respectively. In this case the conventional UPFC has been simulated. The same variables are illustrated in Fig. 13-a and b, but in this case C-UPFC shown in Fig. 9 has been simulated. In both simulations the reference points are the same. As it can be seen, during transient conditions C-UPFC can limit the receiving and sensing ends reactive power flows much better than UPFC. For example, receiving end reactive power flow is limited about 40MVAR in Fig.12-a to 10 MVAR in Fig.13-a and the sending end reactive power is limited about 130MVAR in Fig.12-b to 30MVAR in Fig.13-b. These figures show the reactive power of both ends when the reference point of reactive power is zero and the active power changes as Fig.11. The Fig. 14-a and b describe the reference voltage and current of series and shunt inverters.

To show the capability of C-UPFC for reactive power flow control, step changes of reactive power reference point have been applied to the designed control system. The simulation results are presented in Fig. 15-a and b for reactive power flows of receiving and sending ends. In this case, the load bus voltage and sending end voltage are shown in Fig. 16. This figure shows that CUPFC can properly regulate the load bus voltage. The reference voltages of series inverters and reference current of shunt inverter in this case are given in Fig. 17- a, b and c.

Now we set the line active and reactive power flow reference points to 200 MW and 0 MVAR, respectively. This time the load angle of generator No.2 has been changed as shown in Fig. 18. The simulation results are presented in Fig. 19-a and b. It is obvious that C-UPFC can easily regulate and compensate line active and reactive power flows.

Because, the reference points of active and reactive power of left and right side inverters are same, therefore the reference voltage of these inverters will be same as shown in Fig. 20-a. Fig. 20-b shows the reference current of shunt inverter.

The Fig. 21 shows the DC link capacitors voltages when the line active power flow is changed as Fig. 11. It can be seen that the presented control system for shunt inverter regulates the DC link capacitor voltage as properly.

An attractive application of C-UPFC is load current balancing. The control system shown in Fig.6 has added this capability to the conventional UPFC. The unbalance load has been modeled as shown in Fig.9. The simulation results are illustrated in Fig. 22-a and b. As it can been seen the sending end generator currents are balanced. The injected current by shunt inverter is shown in Fig. 23. Table 1 lists the

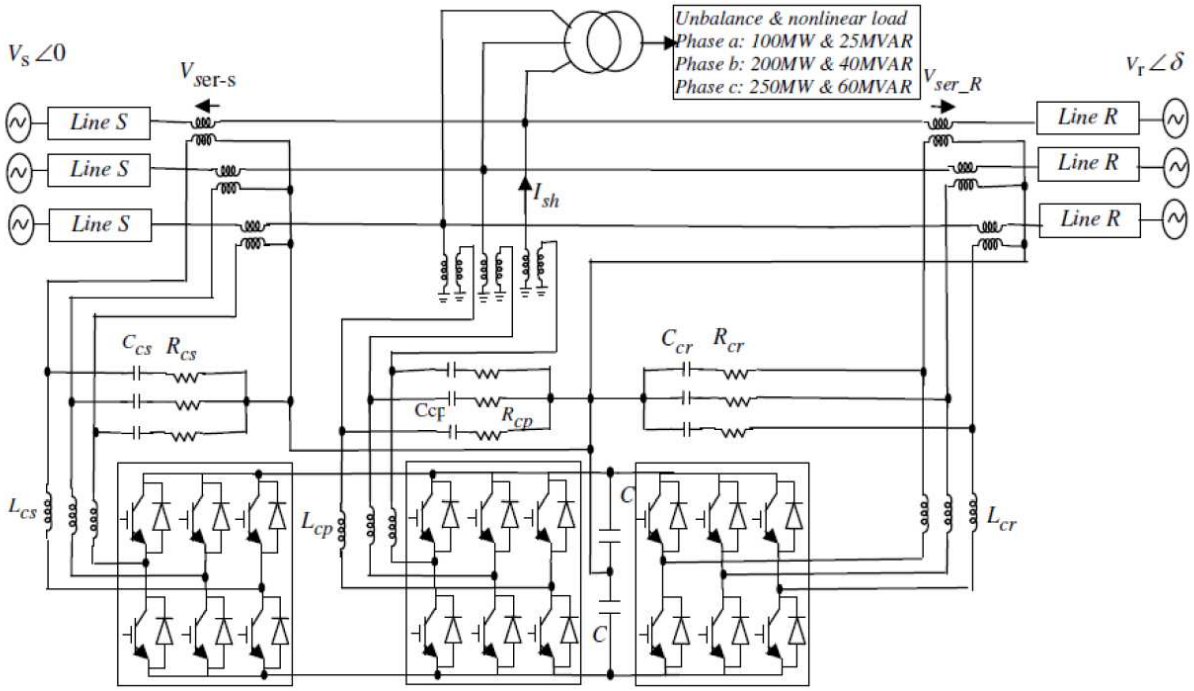

Fig.9: *Configuration of simulation system*

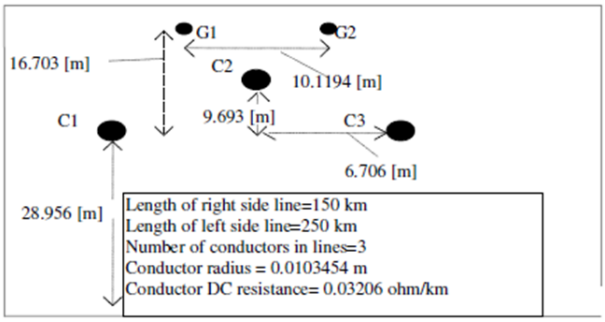

Fig.10: *Transmission lines configuration*

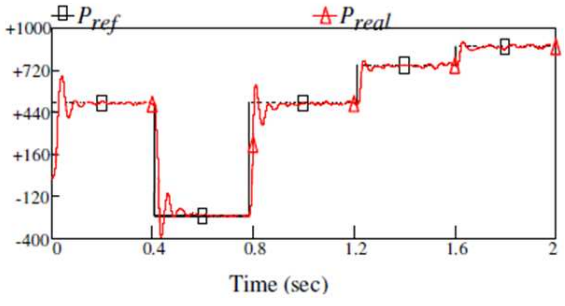

Fig.11: *Reference and active power flow, Q_{ref}=0, C-UPFC installed (MW)*

harmonics and THD of line current when the active and reactive powers are changed as step.

A 3-phase fault through impedance is applied at load bus at 2.5sec. The fault is cleared after 0.075sec. Also it can be seen from waveforms shown in Fig.24 that, the generator at receiving end recovers successfully after clearing the fault. Fig. 24-a shows the line active power when C-UPFC is not installed. Fig. 24-b, c and d show the line active power, load bus voltage and DC link capacitor voltage, when C-UPFC is installed, respectively.

A 3-phase and one phase fault to ground is applied at load bus at 1.5sec and 7sec, respectively. Fig. 25 shows the simulation results of this case. The duration of each fault is considered 0.075sec. The results depicted in Fig.25 show that, the power and phase angle oscillations of generator are quickly controlled and damped faster. Also these results show that, the load bus voltage and DC capacitor voltage are regulated as properly. Fig. 26 and Fig.27 show the injected series voltage by series inverters and injected active and reactive power by shunt inverter at this case.

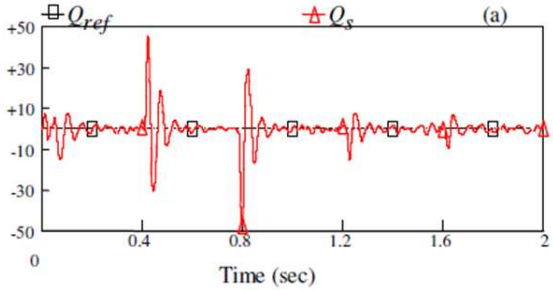

Fig.12-a: *Reactive power of receiving end, Q_{r_ref}=0, UPFC installed (MVAR)*

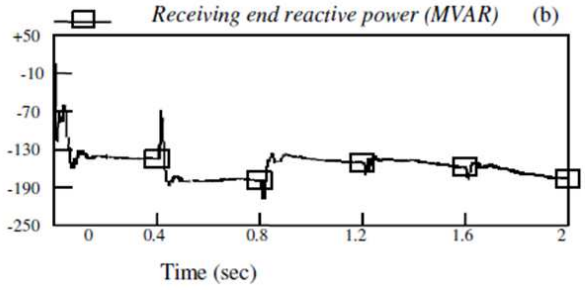

Fig.12-b: *Reactive power of sending ends, Q_{s_ref}, UPFC installed*

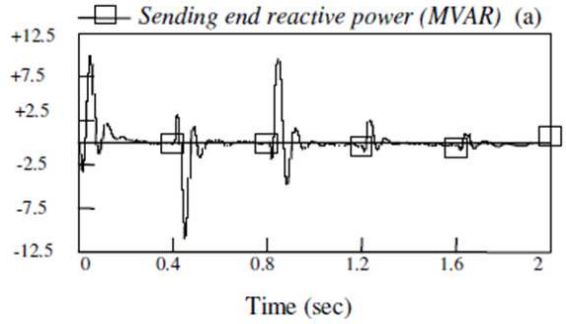

Fig.13-a: *Reactive power of receiving end, Q_{r-ref} =0, C-UPFC installed*

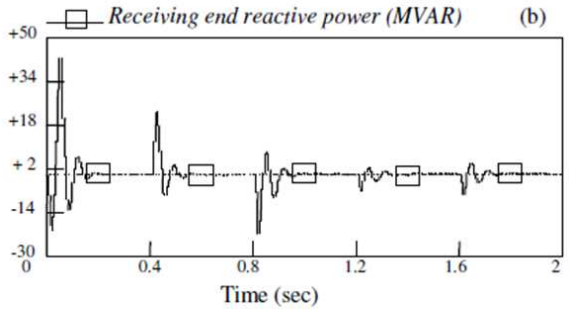

Fig.13-b: *Reactive power of sending end, Q_{s-ref} =0 , C-UPFC installed*

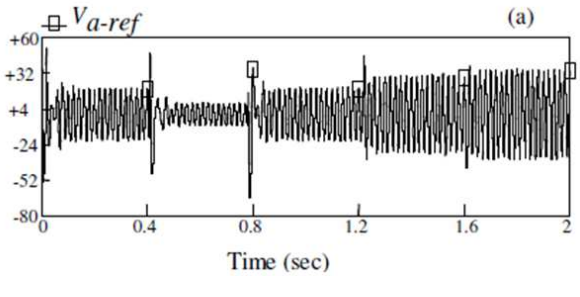

Fig.14-a: *Reference voltage of left and right side inverters*

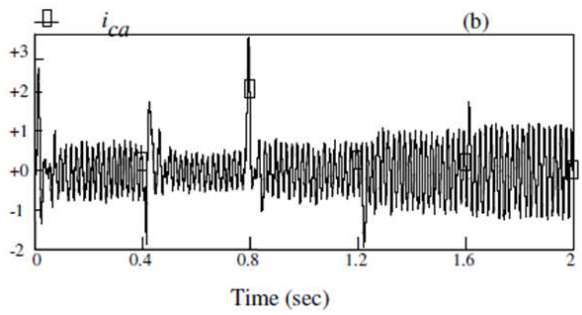

Fig.14-b: *Reference current of shunt inverter*

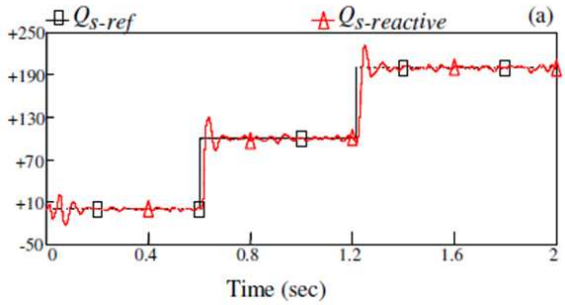

Fig.15-a: *Reference and reactive power flows (MVAR) of sending ends, C-UPFC installed*

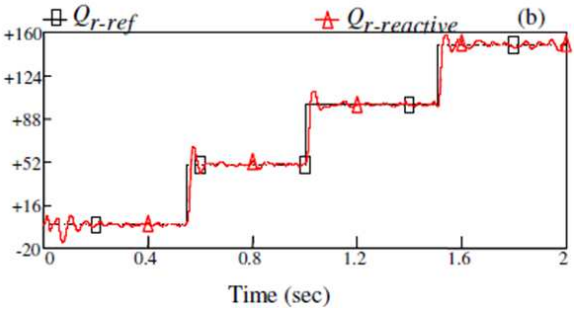

Fig.15-b: *Reference and reactive power flows (MVAR) of receiving C-UPFC installed*

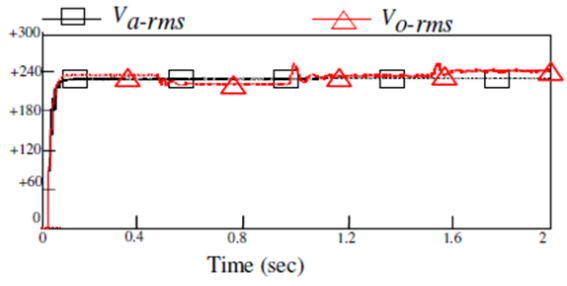

Fig.16: *Sending end and load bus voltage*

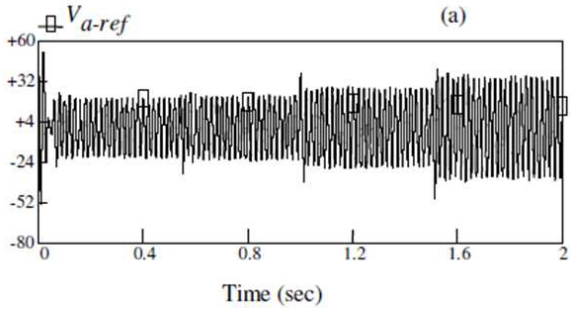

Fig.17-a: *Reference voltage of left side inverter*

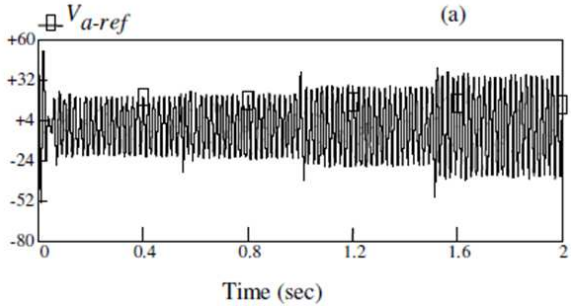

Fig.17-b: *Reference voltage of right side inverter*

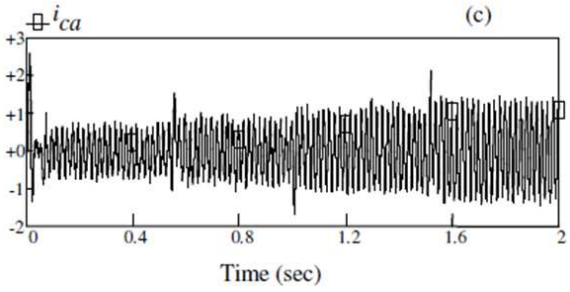

Fig.17-c: *Reference current of shunt inverter*

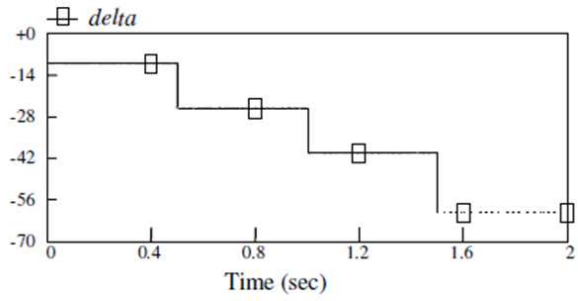

Fig.18: *Step changes of load angle of Gen.2*

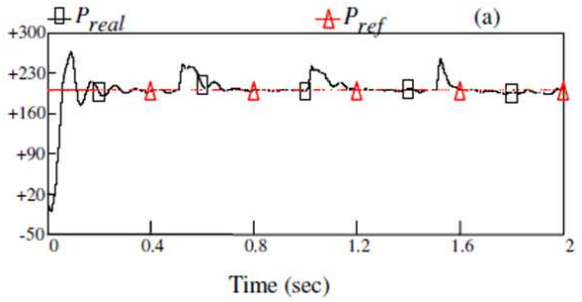

Fig.19-a: *Reference and line active power flow, when load angle of generator 2 has been changed*

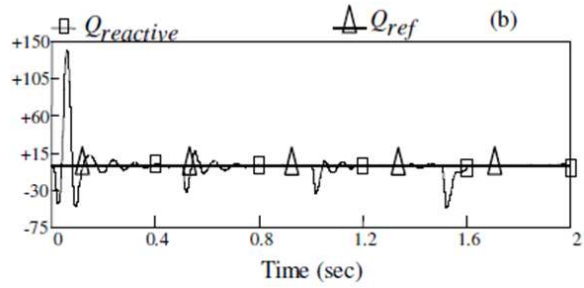

Fig.19-b: *Reference and line reactive power flow, when load angle of generator 2 has been changed*

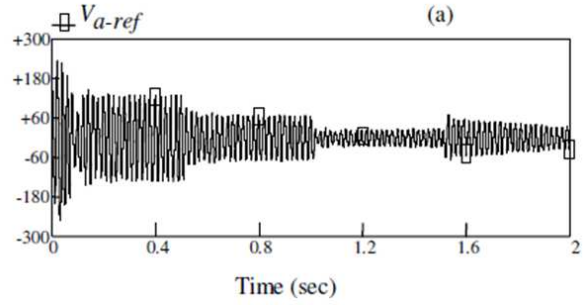

Fig.20-a: *Reference voltage of left & right side inverters*

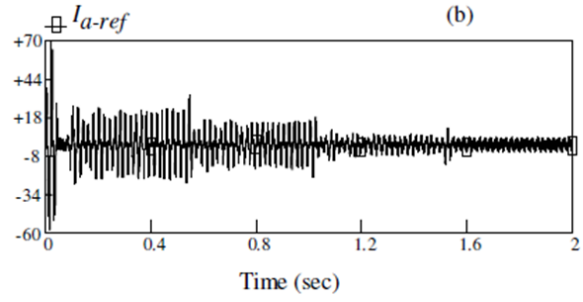

Fig.20-b: *Reference current of shunt inverter*

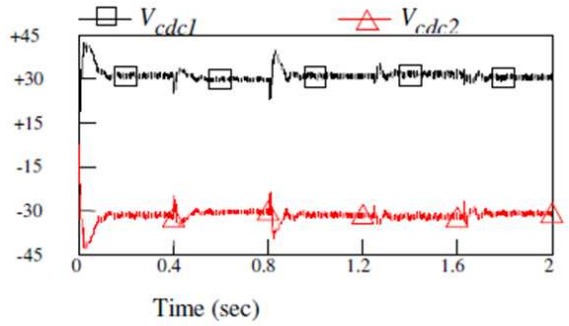

Fig.21: *DC link capacitors voltage*

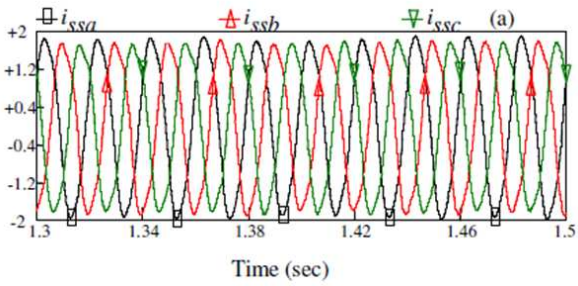

Fig.22-a: *Sending end currents (KA)*

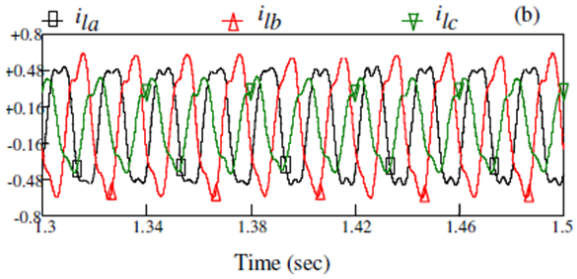

Fig.22-b: *Load side currents (KA)*

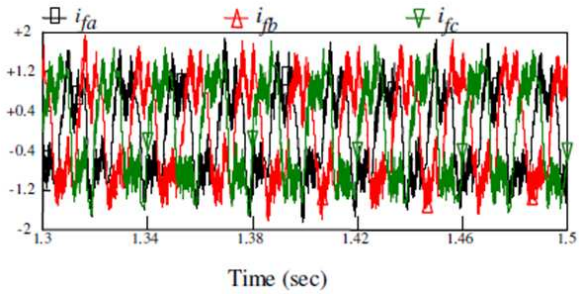

Fig.23: *Injected current by shunt inverter*

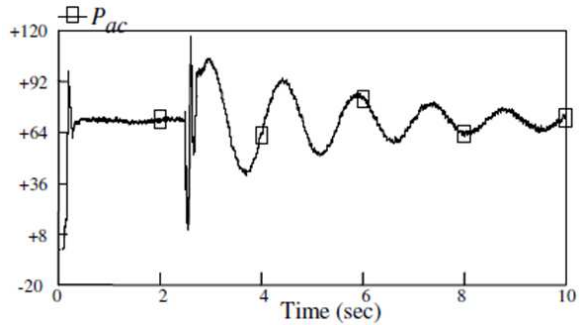

Fig.24-a: *Line active power when a 3-phase fault (through impedance) occurred and C-UPFC is not installed*

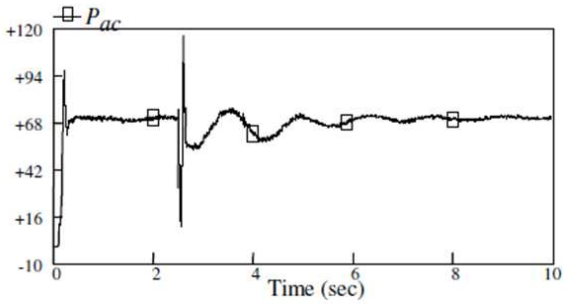

Fig.24-b: *Line active power when a 3-phase fault (through impedance) occurred and C-UPFC is installed*

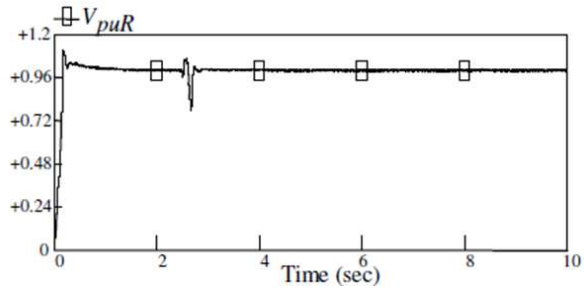

Fig.24-c: *Load bus voltage when a 3-phase fault (through impedance) occurred and C-UPFC is installed*

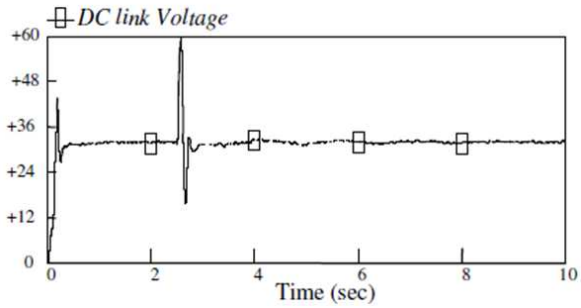

Fig.24-d: *DC link capacitor voltage when a 3-phase fault (through impedance) occurred and C-UPFC is installed*

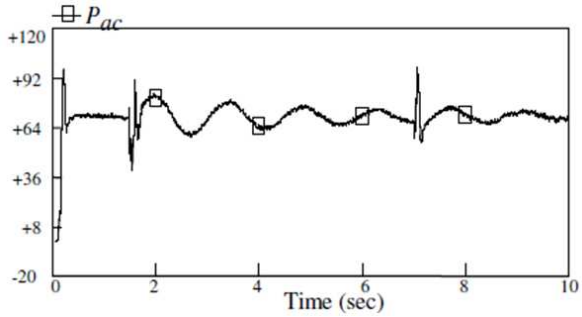

Fig.25-a: *Line active power when a 3 and 1phase faults occurred and C-UPFC is installed*

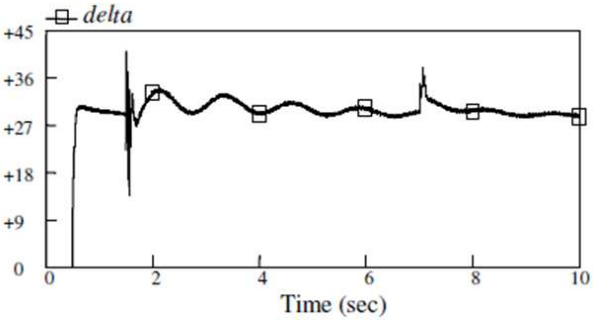

Fig.25-b: *Load angle of generator 2 when a 3 and 1phase faults occurred and C-UPFC is installed*

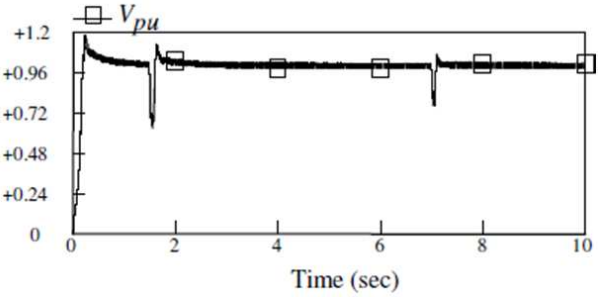

Fig.25-c: *Load bus voltage when a 3 and 1phase faults occurred and C-UPFC is installed*

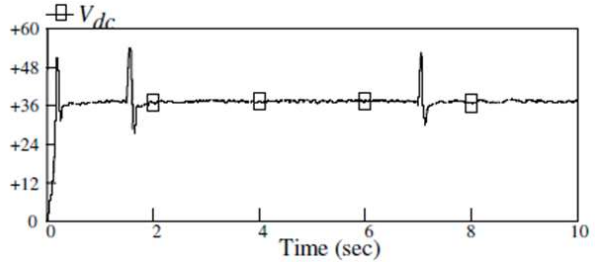

Fig.25-d: *DC link capacitor voltage(KV) when a 3 and 1phase faults occurred and C-UPFC is installed*

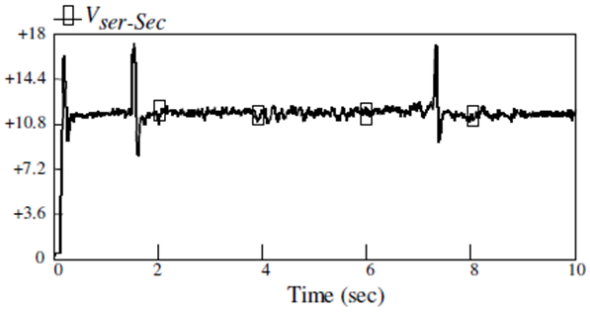

Fig.26: *Inserted series voltage by series inverters when a 3 and 1phase faults occurred and C-UPFC is installed*

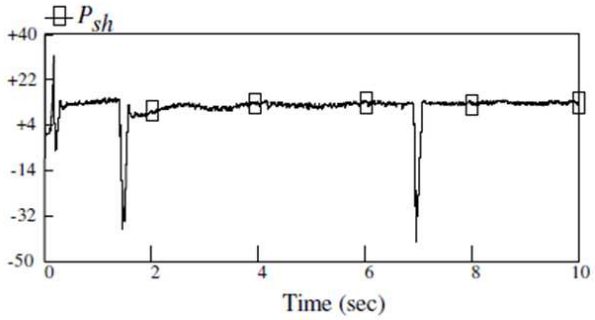

Fig.27-a: *Active power of shunt inverter when a 3 and 1 phase faults occurred and C-UPFC is installed*

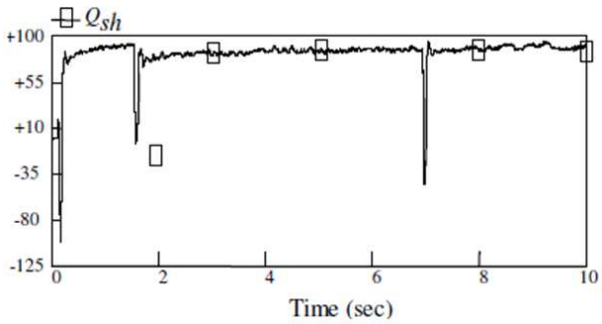

Fig.27-b: *Reactive power of shunt inverter when a 3 and 1 phase faults occurred and C-UPFC is installed*

Table 1: *Table 2: Parameters of C_UPFC*

Harmonics order	3th	5th	7th	11th	13th	THD
Values%	2	1.6	1	.5	.05	2.79

6. CONCLUSION

This paper presents the transient model and control system of a new FACTS device, the center node unified power flow controller (C_UPFC), installed at the midpoint of a transmission line. The presented C_UPFC control system can regulate line active and reactive power flow and voltage at midpoint of the transmission line. The presented control system of C_UPFC not only responses to the step changing in

the active and reactive power, but also is able to exchange the direction of line active power flows. In this paper a supplementary control system is added to the shunt inverter control system to compensate unbalance load current. It shown that presented control system for power oscillation damping is capable to damping the power and rotor angle after 3 and 1 phase fault occurring.

The simulation results indicate the fast dynamic response, validity and effectiveness of the presented new FACTS device and its control scheme.

Appendix

Parameters of generators:
Line to neutral voltage (rms): 11.56 KV
Base angular frequency (rad/sec): 376.991
Armature Resistance (pu): 0.002, 800 MVA
Stator leakage reactance (pu): 0.14
Xd: 1.79 (pu), Xd': 0.169 (pu), Xd": 0.135 (pu)
Xq: 1.71 (pu), Xq': 0.228 (pu), Xq": 0.2 (pu)
Generators out put transformers parameters:
V1/V2 = 20/230 (KV), 900 MVA

Table 2: *Table 2: Parameters of C_UPFC*

Ccp	Lcp	Rcp	Ccs,Ccr	Lcs,Lcr	Rcs,Rcr	C
10μf	2mh	5Ω	10μf	1mh	5Ω	470μf

Parameters of PI controller:

The parameters of PI controller are determined by thorough and repeated study of system responses under various operating conditions. The PI controller settings, which give the best responses under all the tested conditions, are listed bellow:

Kppr1=0.5, Kipr1=0.1, Kpps1=0.09, Kips1=0.5
Kppr2=2.5, Kipr2=1, Kpps2=2.1, Kips2=1.55
Kpqr1=0.45, Kiqr1=0.2, Kpqs1=0.05, Kiqs1=0.7
Kpqr2=2.3, Kiqr2=2.1, Kpqs2=3, Kiqs2=1
Kpv1=0.5, Kiv1=0.2, Kpv2=5, Kiv2=0.2
Kpc1=0.2, Kic1=0.1, Kpc2=1, Kic2=0.1
Parameters of SPWM PI controller:
Kp=100, Ki=1000

References

[1] L. Gyugi, "A Unified Power Flow Control Concept for Flexible AC Transmission Systems," *IEE Proceedings*, Vol.139, No.4, pp. 323-331, July 1992.

[2] Narain G. Hingorani, L. Gyugyi, Understanding FACTs: Concept and Technology of Flexible AC Transmission Systems, IEEE Press, New York, 1999.

[3] C.A. Canizares, Z. Faur, "Analysis of SVC and TCSC Controllers in Voltage Collapse," *IEEE Transactions on PWRS*, Vol.14, No.1, pp. 1-8, Feb. 1999.

[4] Y.Sumi, Y.Harumoto, T.Hasegawa, M.Yano, K.Lkeda, T.Matsuura, "New Static VAR Control Using Force Commutated Inverters," IEEE *Transactions on Power Apparatus and System*, Vol. 100, No. 9, pp.4216-4226, Sept. 1981.

[5] L. Gyugyi, C.D. Schauder, K.K. Sen, "Static Synchronous Series Compensator: A Solid-State Approach to the Series Compensation of Transmission Lines," *IEEE Transactions on Power Delivery*, Vol. 12, No. 1, pp. 406-413, 1997.

[6] K.K.Sen, "SSSC- Static Synchronous Series Compensator: Theory, Modeling Control," *IEEE Trans. On Power Delivery*, Vol. 10, No. 2, pp. 1085- 1097, April 1995.

[7] L. Gyugyi, C.D. Schauder, et al, "The Unified Power Flow Controller: A New Approach to Power Transmission Control," *IEEE Transactions on Power Delivery*, Vol. 10, No. 2, pp. 1085-1093, April 1995.

[8] H. Fujita, Y. Watanabe, H. Akagi, "Control and Analysis of a Unified Power Flow Controller," *IEEE Transactions on Power Electronics*, Vol.14, No.6, pp. 1021-1027, November 1999.

[9] S. Round, Q. Yu, et al, "Performance of a Unified Power Flow Controller Using a d-q Control System," *AC and DC Transmission Conference*, April 1996.

[10] D.G. Cho, E. Ho. Song, "A Simple UPFC Control Algorithm and Simulation on Stationary Reference Frame," *ISIE Conference*, Pusan, Korea, pp.1810- 1815, 2001.

[11] B. Ooi, B. Lu, "C-UPFC: A New FACTs Controller for Midpoint Sitting," *Conference Record of the International Power Electronics Conference*, Tokyo, Japan, pp. 1947-1952, April 2000.

[12] Pranesh Rao, L.M. Crow, Zhiping Yang, "STATCOM Control for Power System Voltage Control Applications," *IEEE Trans. On Power Delivery*, Vol. 15, No. 4, pp. 1311-1317, October 2000.

[13] A. Ajami, S. H. Hosseini, S. Khanmohammadi, G. B. Gharehpetian, "Modeling and Control of C-UPFC for Power System Transient Studies," *Simulation Modelling Practice and Theory*, Vol. 14, p.p.564-576, 2006.

[14] S.H.Hosseini, A. Ajami, "Voltage Regulation and Transient Stability Enhancement of a Radial AC Transmission System Using UPFC," *IECON04*, Pusan, Korea, 2004.

[15] A.Ajami, S.H.Hosseini, "Line Current Balancing Using Unified Power Flow Controller," *TENCON04*, Chiang Mai, Thailand, 2004.

[16] Claudia A. Canizares, Edvina Uzunovic, and John Reeve, "Transient Stability and Power Flow Models of the Unified Power Flow Controller for Various Control Strategies," *Technical Report #2004-09*, University Waterloo, E & EC, March 2004.

[17] P. K. Steimer, H. E. Gruning, J. Werninger, E. Carroll, S. Klaka, and S. Linder, "IGCT A New Emerging Technology for High Power, Low Cost

Inverters," *IEEE Indusry Applications Magazine*, pp. 12-18, July 1999.

[18] PSCAD/EMTDC V4.1, Power System Simulation Software User Manual, Manitoba HVDC Research Center, CANADA, 2003.

Ali Ajami received his B.Sc. and M.Sc. degrees from the Electrical and Computer Engineering Faculty of Tabriz University, Iran, in Electronic Engineering and Power Engineering in 1996 and 1999, respectively, and his Ph.D. degree in 2005 from the Electrical and Computer Engineering Faculty of Tabriz University, Iran, in Power Engineering. His main research interests are dynamic and steady state modelling and analysis of FACTS devices, harmonics and power quality compensation systems, microprocessors, DSP and computer based control systems.